An Automated Field-Circuit Coupling Simulation Method Based on PSpice-MATLAB-COMSOL for SiC Power Module Design

Yayong Yang, *Student Member, IEEE*, Zhiqiang Wang, *Senior Member, IEEE*, Yuxin Ge, *Student Member, IEEE*, Guoqing Xin, *Member, IEEE*, and Xiaojie Shi, *Senior Member, IEEE*

***Abstract*—Multiphysics simulation software is indispensable for silicon carbide (SiC) power module design. Lacking interface between circuit simulation software and thermal-fluid-mechanical simulation software poses challenges for accurate design of the power modules. In this article, an automated field-circuit coupling simulation method based on the self-developed COMSOL-PSpice interface software is proposed to achieve precise and fast multiphysics cosimulation of multichip SiC power modules. First, the multiphysics coupling mechanism of SiC power modules is analyzed to reveal that the precise and timely data transfer between temperature and power loss is crucial to enabling an accurate multisoftware cosimulation. To realize the automatic data transfer between COMSOL and PSpice, a MATLAB-based software interface is developed. Then, a multirate and indirect coupling strategy is proposed to improve the simulation accuracy of the developed COMSOL-PSpice software interface and speed up the cosimulation process. To break the limitations of the indirect coupling strategy on simulation accuracy and efficiency with fixed time steps, a variable time step coupling analysis method based on the numerical solution of temperature coupling state variables is proposed. Finally, the proposed field-circuit coupling cosimulation method is verified by simulation and experiment results from a buck converter. The comparison between simulation and experimental results demonstrates the validity of the developed cosimulation interface software, which gives a mismatch below 5% and simulation efficiency 3–5 times higher, if compared to that using fixed time steps.**

***Index Terms*—COMSOL-PSpice, field-circuit coupling, multiphysics simulation, SiC power modules, software interface.**

Manuscript received 14 March 2023; accepted 24 June 2023. Date of publication 7 July 2023; date of current version 1 September 2023. This work was supported in part by the National Natural Science Foundation of China under Grant 52277179 and in part by Hubei Jiufengshan Laboratory. Recommended for publication by Associate Editor K. Wada. *(Corresponding authors: Zhiqiang Wang; Xiaojie Shi.)*

Yayong Yang is with the Institute of Artificial Intelligence, Huazhong University of Science and Technology, Wuhan 430074, China (e-mail: yangyayong@hust.edu.cn).

Zhiqiang Wang, Yuxin Ge, Guoqing Xin, and Xiaojie Shi are with the School of Electrical and Electronic Engineering, Huazhong University of Science and Technology, Wuhan 430074, China (e-mail: zhiqiangwang@hust.edu.cn; geyuxin0324@hust.edu.cn; guoqingxin@hust.edu.cn; xiaojie_shi@hust.edu.cn).

Color versions of one or more figures in this article are available at https://doi.org/10.1109/TPEL.2023.3293162.

Digital Object Identifier 10.1109/TPEL.2023.3293162

I. Introduction

MOTIVATED by high power density, high efficiency, silicon carbide (SiC) power semiconductor modules become more and more popular for industrial applications, such as electric vehicle and multielectric/all-electric aircraft [1], [2]. On the other hand, whether SiC power modules can be fully utilized to maximize the power density and efficiency of converters depends on their packaging design [3], which heavily relies on the simulation software to characterize the corresponding physical quantities. The accuracy of the corresponding physical parameters extraction, such as chip junction temperature and loop parasitic inductance, will affect the performance of SiC power modules and heatsinks. With low simulation accuracy, the design will likely be too conservative for reliability, which impedes the improvement of power density. This situation, however, frequently occurs with the single physical field simulation, due to complex coupling relationships of multiphysics in power modules. To guarantee sufficient simulation accuracy, multiphysics cosimulation considering complicated coupling relationships becomes critical for the design of power modules.

The multiphysics that need to be considered during power module design typically involves electric, magnetic, fluid, thermal, and mechanical. To realize the electro-thermal multiphysics cosimulation, a reduced-order zero-dimensional (0-D) thermal impedance network model can be obtained by 3-D finite element thermal simulation results or experimental results [4]. Then, the acquired thermal impedance network model can be used for electro-thermal cosimulation in the circuit simulation software (PSpice, LTspice, Saber, Simulink). A dedicated interface tool is provided in ANSYS Icepak to realize the conversion from 3-D thermal simulation to the 0-D Foster or Rational function thermal network model, which can later be used for electro-thermal coupling simulation in ANSYS Twin Builder [5], [6]. However, the following problems remain when employing ANSYS to perform the multiphysics cosimulation of SiC power modules.

1) When importing bare die SiC MOSFETS spice models from power device manufacturers (e.g., Infineon, CREE, ROHM) into ANSYS Twin Builder, an error message often shows up, causing an unstable use of spice models provided by the manufacturers.

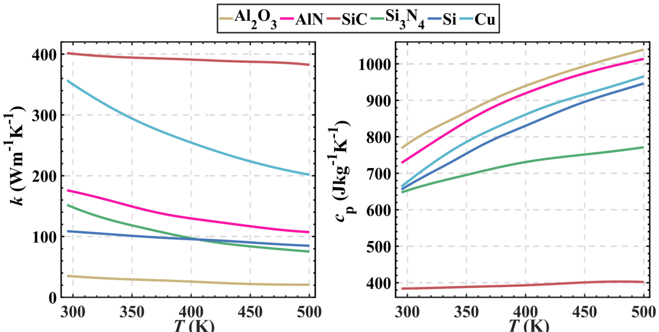

Fig. 1. Temperature sensitivity of thermal parameters for commonly used packaging materials [7].

2) As shown in Fig. 1, the thermal conductivity properties of packaging materials change significantly with temperature. The thermal network generated by the ANSYS Icepak interface tool can cause unsatisfactory cosimulation accuracy due to the neglect of the temperature dependence of packaging materials.
3) Moreover, in ANSYS, the lack of the bidirectional coupling interface between circuit simulation software and thermal-mechanical simulation software makes the direct coupling simulation of the lumped circuit and thermal-mechanical field difficult.

Another commercial multiphysics simulation software COMSOL also has problems when applied to multiphysics cosimulation. The circuit simulation module, ac–dc Module, does not support importing the device spice model. Besides, the coupling interface of the ac–dc Module and Heat Transfer Module is not available in COMSOL.

In general, the simulation capability of single multiphysics simulation software is limited, resulting in low simulation accuracy. To deal with the above problems, several multiphysics cosimulation approaches have been proposed, which can be divided into the following two types. The first type still relies on a single simulation software platform. In [8] and [9], mathematical expressions between the device power loss and temperature are derived through proper simplification, skipping the process of circuit simulation to calculate the power losses of devices. Then, the derived mathematical expressions serve as the boundary condition for COMSOL thermal and mechanical finite element simulation. This simplified derivation method is difficult to obtain the precise loss, resulting in low simulation accuracy. A similar method has also been explored in [10], in which an uneven power loss derivation model is utilized. Moreover, a method based on the current module in COMSOL is proposed in [11]. It inputs the fixed power loss in the heat source input box as the switching loss of the chip while the Joule heat generated by the sinusoid current flowing in power modules is regarded as conduction loss. However, the current law of switch circuits is complicated, and it is hard to express the current change by a sine function. Meanwhile, the fixed switching loss setting ignores the effect of temperature dependence, which reduces simulation accuracy. As a compromise between the accuracy and efficiency of simulation, a thermal modeling tool based on the finite difference method is proposed in [7]. Utilizing this tool, a 3-D equivalent thermal network model considering the effect of temperature can be imported into the LTspice simulator for electro-thermal co-simulation. This method achieves a trade-off between simulation accuracy and speed, with relatively faster simulation speed but lower accuracy, if compared to the finite element thermal simulation, due to the simplified 3-D thermal model that considers temperature dependence.

The second type is multisoftware collaborative multiphysics cosimulation, which typically involves the commercial multisoftware cosimulation platform Isight, due to its powerful multi-parameter and multidisciplinary cosimulation and optimization. Isight provides interfaces for a large number of third-party software in the form of application components to realize data flow among various software [12]. Nevertheless, the following issues arise when utilizing Isight to achieve electrical-thermal-mechanical cosimulation. Application components of COMSOL and common circuit simulation software (PSpice, LTspice, Saber) are not yet available in Isight, which means that they cannot exchange data with Isight currently. Though the software interface can be developed via the application component named Simcode in Isight, the developed software interface does not allow for the transient simulation states inheritance. This limitation makes transient electro-thermal-mechanical cosimulation difficult to be implemented in Isight. To solve this issue, some multisoftware-based approaches have been proposed. In [13] and [14], a direct field-circuit coupling simulation method based on circuit simulation software PSpice and thermal simulation software ANSYS Icepak is presented to perform transient short-circuit conditions simulation. Through data exchange between power losses (simulated by PSpice) and temperature (simulated by Icepak) monitored by MATLAB script, more accurate electro-thermal cosimulation results are obtained for short-circuit conditions. However, the fixed data exchange time step makes it difficult for steady-state simulations because of the complicated and time-consuming calculation, which greatly limits the application of this method. For power module design and other applications, steady-state results are of greater concern in most cases. In addition, the parasitic parameters introduced by electromagnetic coupling and parallel chips temperature difference are not considered in this method, which negatively affects the simulation accuracy. Moreover, the thermal-mechanical coupled simulation cannot be performed in ANSYS Icepak, hence, no mechanical stress is involved. To break this limitation, an analogous field-circuit coupling simulation method based on PSpice-COMSOL is presented in [15]. By utilizing the coupling between the Heat Transfer Module and Solid Mechanics Module in COMSOL, a field-circuit coupled electro-thermal-mechanical cosimulation is available. However, other issues described in [13] and [14] are still unresolved.

To solve the unresolved issues, this article proposes an automated field-circuit coupling simulation method based on the self-developed software interface with an adaptive data exchange time steps adjustment strategy, which is suitable for both steady-state and transient simulation. Moreover, this method takes into consideration the effects of parasitic parameters and

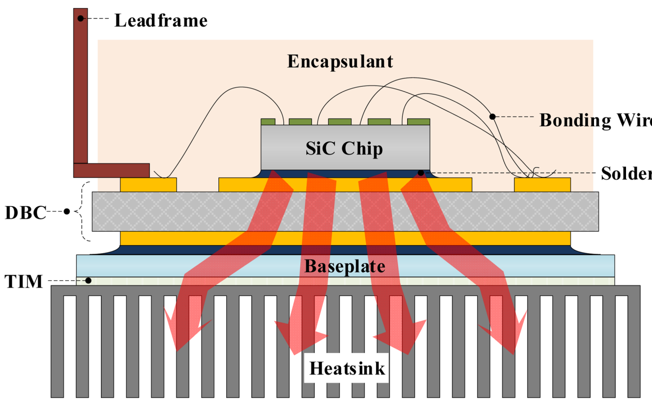

Fig. 2. Typical wire-bonded power modules configuration.

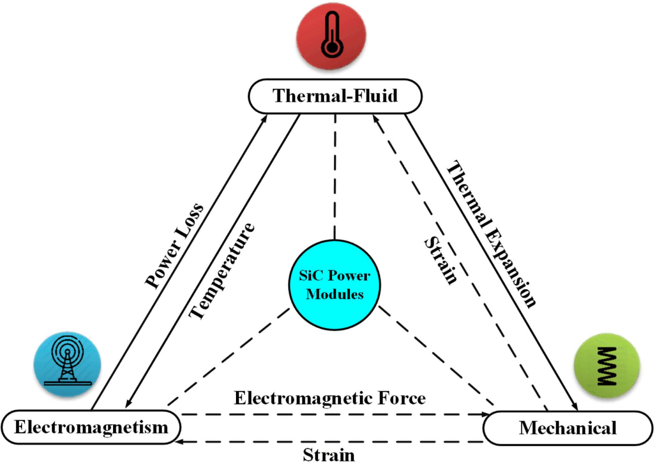

Fig. 3. Multiphysics coupling mechanisms in SiC power modules.

temperature distribution differences in multichip SiC power modules.

The rest of this article is organized as follows. Section II presents the field-circuit coupling software interface development process and coupling strategy. Based on the developed software interface, the strategy to balance simulation accuracy and speed is proposed in Section III. In Section IV, the simulation accuracy and speed of the proposed interface-based cosimulation software platform for a buck inverter is validated by comparing it to experimental results. Finally, Section V concludes this article.

II. Development of Field-Circuit Coupling Software Interface

In this section, the multiphysics coupling mechanism of SiC power modules is analyzed to reveal the coupling strength. Based on the full consideration of coupling relationships, a MATLAB-based software interface is developed. To realize an efficient variable data exchange, a multirate and indirect coupling strategy is applied to the software interface. Detailed analysis and development flow are demonstrated as follows.

A. Multiphysics Coupling Mechanism of SiC Power Modules

The typical SiC power module configuration is shown in Fig. 2. When current flows through SiC power chips, power losses will occur, causing SiC chip temperature to rise. Temperature changes will affect the electrical characteristics of the chips, which in turn will change power losses. In addition, in the process of heat transfer from the chips to the heatsink through the direct-bonded copper (DBC), thermal interface material, and baseplate, mechanical stress will appear inside power modules due to the mismatched thermal expansion coefficient of different packaging materials. It can be seen that complex multiphysics coupling relationships exist in power modules, as illustrated in Fig. 3, for SiC power modules.

The strength of the coupling relationship determines whether this coupling needs to be considered in the multiphysics simulation. Electro-magnetic, thermal-fluid, electro-thermal, and thermal-mechanical couplings are strong, while fluid-solid and electromagnetism-mechanical couplings are weak and can be neglected [16], [17], [18], [19], as marked by the solid (strong coupling) and dashed (weak coupling) arrows in Fig. 3. The abovementioned coupling relationship needs to be fully considered in the simulation design of power modules.

B. Multiphysics Cosimulation Software Interface Development

The key to realizing an accurate coupling simulation between different physical fields relies on the transfer of corresponding coupling variables through a multiphysics coupling interface. Electromagnetic coupling simulations can be implemented by lumped circuits built with parasitic parameter networks derived from Q3D. The fluid-thermal coupling can be realized through the Nonisothermal Flow multiphysics coupling interface in COMSOL. Similarly, the thermal-mechanical coupling can be accomplished through the Thermal Expansion multiphysics coupling interface in COMSOL to transfer coupling variables. However, the circuit and thermal field coupling interface is not yet commercially available.

Considering the coupling interface of commercial software and the coupling relationships among multiphysics, a MATLAB-based software interface development method for power modules multiphysics cosimulation is developed to realize field-circuit coupling simulation between 3-D fluid-thermal-mechanical field and 0-D circuit, as illustrated in Fig. 4. The proposed multisoftware cosimulation framework consists of three parts: the circuit model constructed by spice language in PSpice, the fluid-thermal-mechanical model built by Java language in COMSOL, and the script program written in MATLAB. MATLAB serves as an interface to coordinate data exchange between PSpice circuit simulation and COMSOL fluid-thermal-mechanical simulation, breaking the incompatibility between data from PSpice and COSMOL.

The existing software interface in COMSOL (LiveLink for MATLAB) can link COMSOL to the MATLAB scripting environment. For each operation performed in COMSOL, the corresponding Java command is automatically generated via this interface. Conversion of COMSOL operational steps into Java command code, allows MATLAB to control the entire

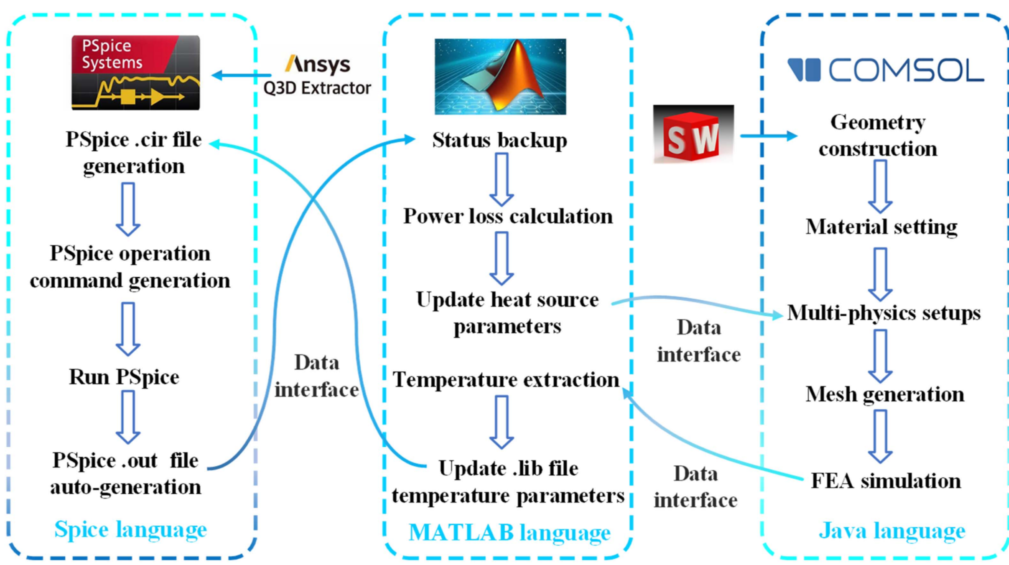

Fig. 4. Proposed multisoftware cosimulation framework.

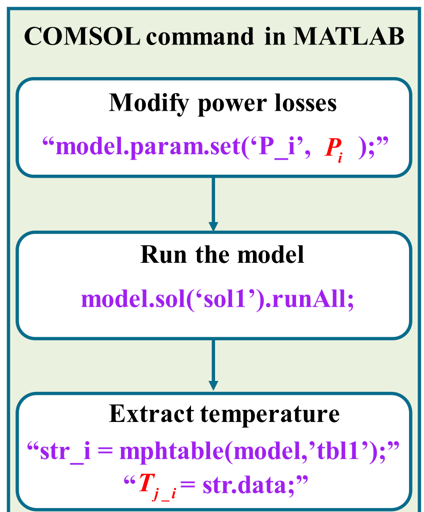

Fig. 5. Method of data interaction between MATLAB and COMSOL.

Fig. 6. Flowchart of the development of the data interaction interface between MATLAB and PSpice.

simulation modeling process, which can facilitate the data interaction between MATLAB and COMSOL, as shown in Fig. 5. On the other hand, the automatic data exchange interface between MATLAB and PSpice is not yet available.

To address this issue, an interface program based on the flowchart depicted in Fig. 6 is developed. The MATLAB system command controls the execution of the circuit input file (file with the .cir suffix) and invokes the PSpice A/D solver for circuit simulation model calculations. After the input file is executed in PSpice A/D (circuit simulator), the output file with the .out suffix will generate automatically. By making corresponding settings in the command part of the input file, the .out file will contain the power loss data information of each heat source. The extracted power loss data can be processed by corresponding functions in MATLAB to obtain the average power loss of each heat source over a period of time. The power loss data obtained by MATLAB can then be transferred to COMSOL as the boundary condition of heat source input for thermal simulation, via the interface with COMSOL. In this way, the automatic transfer of PSpice simulation data to COMSOL is achieved.

The transfer of extracted temperature data to PSpice means that the data is transferred to the spice model or temperature-related parameters, as depicted in Fig. 7. For bare die diodes and bare die MOSFETs without junction temperature pin, the junction temperature data is assigned to the absolute temperature command line written in the spice model file in advance by using text search and replace commands. In this way, current temperatures of bare dies will override the circuit global temperature specification. For bare die MOSFETs with junction temperature pin, when configuring the circuit simulation, the junction temperature pin can be directly connected to the controllable dc voltage source. Considering the junction temperature value

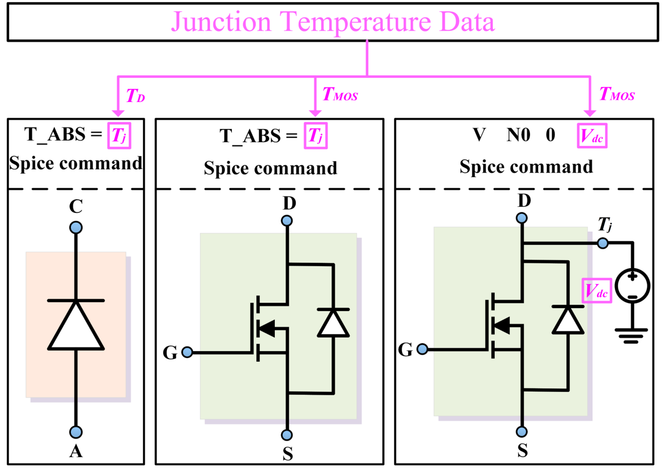

Fig. 7. Method of transferring junction temperature data extracted by MATLAB to PSpice.

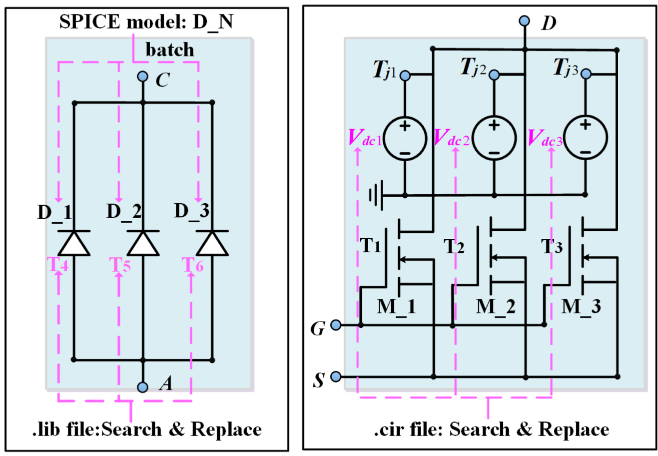

Fig. 8. Method of transferring temperature data when the junction temperature of parallel multichip is different.

as the voltage value on these dc voltage sources, temperature data transfer from MATLAB to PSpice can be accomplished, by updating the voltage values of the junction temperature pin in real-time.

The abovementioned method can be extended to deal with the temperature difference among multiple chips, as caused by unbalanced chip characteristic parameters, package layout, gate drive circuit asymmetry, and other reasons. As indicated in Fig. 8, when the temperature data of multiple parallel chips is transferred to the diode spice model, the same device model can first be batch named using the batch command to obtain multiple models with different file names. Then, models with different file names are processed separately to realize the respective temperature data transfer. For bare die MOSFET models without junction temperature pin, the method is similar. When the temperature data is passed to the bare die MOSFETs with junction temperature pin, each chip junction temperature pin needs to be connected to a separate dc voltage source for separate temperature transfer. The method of temperature transfer separately enables simulation of the same circuit at different device temperatures without all device temperatures being set to the same in the circuit.

The abovementioned interface development method can realize the automatic data transfer between PSpice and COMSOL, and overcome the problem of insufficient simulation capability of a single software.

C. Multirate and Indirect Interface Coupling Strategy of Software Interface

Efficient and accurate transfer of simulation data between PSpice and COMSOL requires a suitable coupling strategy. Bidirectional indirect sequential coupling is adopted in the developed software interface to maximize the advantages of mature commercial simulation software and reduce model complexity and solution cost [20], as indicated in Fig. 9. In the proposed coupling strategy, a simulation data iteration cycle consists of four steps.

Step 1: The transient circuit simulation at a given temperature is performed in PSpice. The circuit simulation is suspended when the data exchange time is reached, as defined as PSpice time steps in which data is exchanged for COMSOL (PTSC). The given temperature of the first iteration is the ambient temperature while that for the second and subsequent iterations is determined by the temperature delivered by COMSOL.

Step 2: MATLAB processes the circuit simulation output file to obtain the average power loss of each heat source. Then, the power loss is communicated to COMSOL through the developed software interface. The boundary condition (input power loss) for thermal-mechanical simulations in COMSOL is updated.

Step 3: The transient thermal-mechanical simulation with a given power loss is carried out in COMSOL. The thermal-mechanical simulation is suspended when the data exchange time is reached, as defined as COMSOL time steps in which data is exchanged for PSpice (CTSP). The simulated power loss of the heat source is obtained by PSpice.

Step 4: MATLAB extracts the maximum value of the heat source temperature at this moment from the simulation file. The maximum temperature is then fed back to the PSpice circuit model as the new temperature boundary condition.

Following the iterative process previously, the loop iteration will be performed continuously until each physical field reaches the equilibrium state, and the system convergence solution is obtained. Depending on the research purpose, different iteration termination conditions are required. For transient problems, the simulation terminates when the corresponding simulation time is reached. For steady-state problems, the iterative termination criterion adopted in this article is: the relative temperature decline between two consecutive iterations is less than the set minimum.

In the process of iteration cycle, two successive iterative processes are closely related. To realize the dynamic and continuous simulation, states of each physical field at the end of the previous cycle will serve as the initial states of the next cycle (state inheritance), and the simulation continues under new boundary conditions. This article utilizes restart analysis for COMSOL

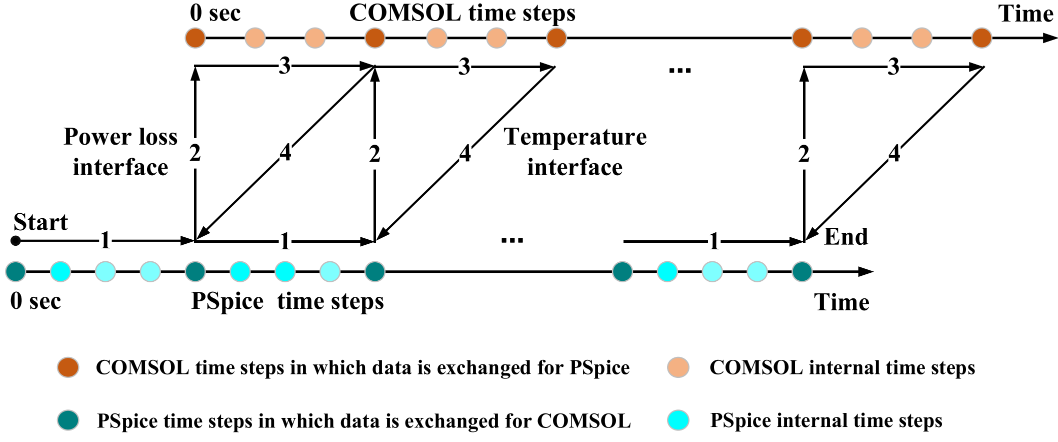

Fig. 9. Multirate and indirect interface coupling strategy adopted by the proposed cosimulation method.

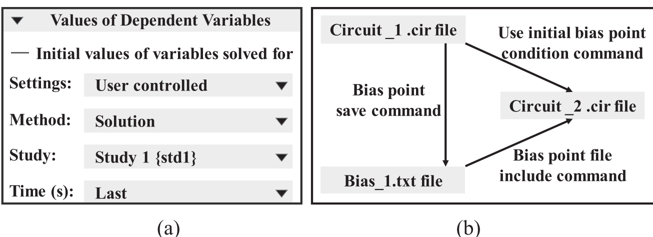

Fig. 10. Approach to implement state inheritance in COMSOL and PSpice. (a) COMSOL. (b) PSpice.

and PSpice to achieve simulation state inheritance, as shown in Fig. 10. In COMSOL, the inheritance of thermal and mechanical simulation states is achieved by setting the solution at the last time point to the initial value of the solution variable. In PSpice, a variety of commands related to bias points are combined to implement the inheritance of circuit simulation states.

Steps 1 and 3 of each cycle also exist in close relationships, except for two successive iterative processes. PTSC should align with CTSP in the same iterative process. This is because the operating time of each physical field is equal, so the time steps in each corresponding transient simulation need to match.

Depending on the simulation purpose, different PTSC and CTSP can be set to realize multirate multiphysics coupling simulation. In short time scale simulations, such as short circuit simulations, where the electrical, thermal, and mechanical characteristics of the power module change dramatically in a short time period, PTSC and CTSP need to be set at the ms level [15]. For long time events, such as steady-state simulations, PTSC and CTSP can be at the seconds level to obtain a good balance between accuracy and computational efficiency. When the simulation system reaches a steady state, ms level PTSC and CTSP can be set to observe the transient junction temperature fluctuation. On the other hand, PSpice internal time steps (PITS) adopted by the circuit simulator to solve transient circuit simulation are much smaller than COMSOL internal time steps (CITS) for transient thermal-mechanical simulation. To ensure accurate simulation of the switching behavior and power loss, ns level PITS are generally required in PSpice. The time scale of heat transfer, however, is ms level, ms level CITS is adequate for high-precision simulation of thermal and mechanical in COMSOL.

Following the strict logical relationship, the indirect and bidirectional coupling strategy enables coupling simulation of the dynamic heat transfer and electrical characteristics of power modules. This solves the converge problems that normally occur in complex multiphysics cosimulation.

III. Adaptive Time Step Adjustment Method of Interface-Based Cosimulation

A. Strategy of Time Step Adjustment

In the indirect sequential coupling solution process, since other coupling fields are ignored in the solution CTSP interval, residuals exist in each CTSP. Excessive residuals will jeopardize the convergence of the numerical integration. To address this issue, a very small and fixed iterative time step is generally adopted to ensure the accuracy and stability of the iterative solution [21]. However, a small CTSP will inevitably lead to more iterations and lower computing efficiency. A large CTSP can reduce the number of iterations, but it may cause a larger truncation error [22]. In summary, it is difficult to balance the accuracy and efficiency by using a fixed CTSP in the proposed multisoftware cosimulation, as shown in Fig. 11.

To solve the problem of fixed CTSP, an adaptive CTSP analysis method based on the numerical solution of temperature coupling state variables (TCSV) is proposed. Since, it is difficult to obtain analytical expressions of TCSV, a three-point derivation formula based on the Lagrangian interpolation polynomial ($L_n(t)$) is established by extracting the TCSV of three consecutive iterative time points, as shown in Fig. 12.

The numerical curve in the simulation time domain $[t_0,\ t_n]$ is recorded as $y = \emptyset(x)$. The corresponding temperature numerical solutions at three consecutive data exchange time points $t_i,\ t_{i+1} = t_i + \lambda_i$, and $t_{i+2} = t_i + \lambda_{i+1} + \lambda_{i+2}$ are recorded as $T(t_i)$, $T(t_{i+1})$, and $T(t_{i+2})$. Then, the following expression

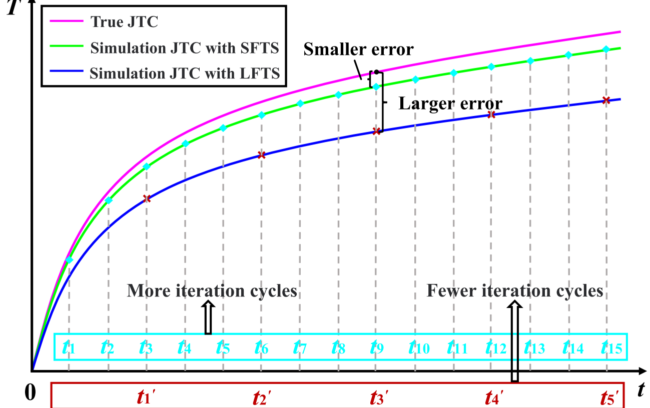

Fig. 11. Schematic diagram of the drawback existing with a fixed CTSP. (JTC means Junction temperature curve, LFTS means large and fixed time steps while SFTS stands for small and fixed time steps.).

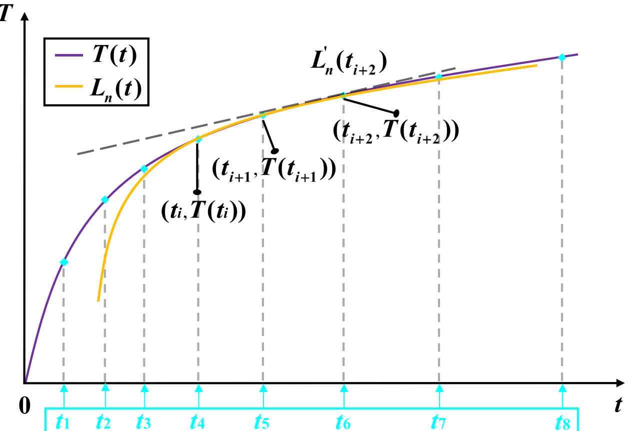

Fig. 12. Schematic diagram of interpolation polynomial construction.

can be obtained by constructing a quadratic Lagrangian interpolation polynomial and taking its first-order derivative:

$$L_n'(t) = \frac{(t-t_{i+1})+(t-t_{i+2})}{\lambda_{i+1}(\lambda_{i+1}+\lambda_{i+2})}T(t_i) - \frac{(t-t_i)+(t-t_{i+2})}{\lambda_{i+1}\lambda_{i+2}}T(t_{i+1}) + \frac{(t-t_i)+(t-t_{i+1})}{\lambda_{i+2}(\lambda_{i+1}+\lambda_{i+2})}T(t_{i+2}). \quad (1)$$

Taking time t_{i+2} as the current time point, substituting into (1), and supposing $i = i + 2$, the first-order variable-step differential formula can be expressed as

$$L_n'(t_i) = \frac{\lambda_i}{\lambda_{i-1}(\lambda_{i-1}+\lambda_i)}T(t_{i-2}) - \frac{\lambda_{i-1}+\lambda_i}{\lambda_{i-1}\lambda_i}T(t_{i-1}) + \frac{\lambda_{i-1}+2\lambda_i}{\lambda_i(\lambda_{i-1}+\lambda_i)}T(t_i). \quad (2)$$

Equation (2) is the judgment formula for the adaptive adjustment of each CTSP. The first-order derivative of the interpolation function at the current time point is calculated by solving (2), and the CTSP adjustment strategy illustrated in Fig. 13 is established accordingly. Note that the time steps judgment threshold interval

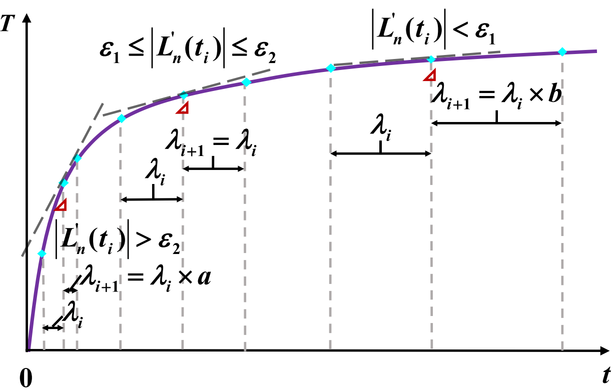

Fig. 13. Schematic diagram of the adaptive CTSP adjustment strategy.

is $[\varepsilon_1, \varepsilon_2]$. In this interval, the slope of the coupling state variable T_i response curve needs to be estimated, and conduct multiple tests and step-by-step corrections to adjust. Note that the CTSP adjustment coefficients are a and b, respectively, where $a \in (0, 1)$, $b \in (1, +\infty)$.

1) If $|L_n'(t_i)| \in [\varepsilon_1, \varepsilon_2]$, then let $\lambda_{i+1} = \lambda_i$.
2) If $|L_n'(t_i)| < \varepsilon_1$, then let $\lambda_{i+1} = \lambda_i \times b$. Under this condition, the temperature change is relatively mild, and the residual error is small. CTSP can be appropriately increased to improve the efficiency of the solution.
3) If $|L_n'(t_i)| > \varepsilon_2$, then let $\lambda_{i+1} = \lambda_i \times a$. In this case, the temperature changes sharply. Time steps with short interval may cause a large residual error. Therefore, CTSP should be minimized to ensure the accuracy of the solution.

As described previously, the adaptive adjustment strategy is adopted during the iteration to dynamically adjust the CTSP according to the curve slope of temperature coupling variables. The range of CTSP can be determined as follows.

B. Range of Time Steps

Taking the first derivative of the interpolation remainder of the Laplace interpolation polynomial, the following expression can be obtained:

$$R'(t) = \emptyset'(t) - L_n'(t) = \frac{\emptyset^{(n+1)}(\xi)}{(n+1)!}\omega'(t) + \frac{\omega(t)}{(n+1)!}\frac{d}{dt}\emptyset^{(n+1)}(\xi). \quad (3)$$

When solving the derivative value at the time point $t_k, t = t_k$, $\omega(t_k) = 0$, so the second term on the right side of (3) is 0. Accordingly, the following expression can be obtained:

$$R'(t) = \frac{f^{(n+1)}(\xi)}{(n+1)!}\omega'(t) = \frac{\emptyset^{(3)}(\xi)}{6}\omega'(t). \quad (4)$$

Substituting adjacent iterative nodes into (4), the following expression can be obtained:

$$R'(t) = \frac{\lambda_{i+1}(\lambda_{i+1}+\lambda_i)}{6}\emptyset^{(3)}(\xi). \quad (5)$$

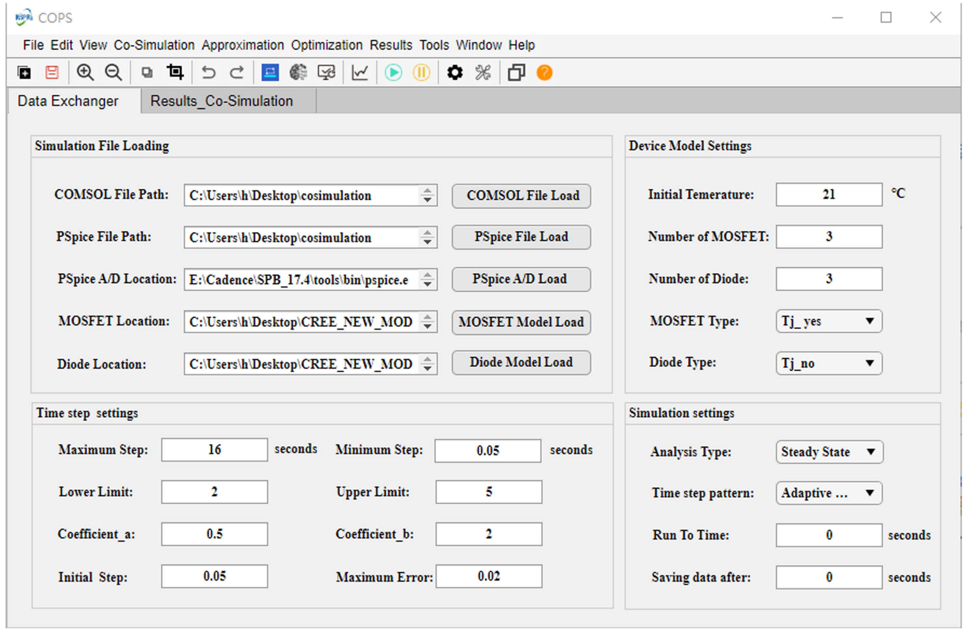

Fig. 14. Self-developed interface software user interface.

Equation (5) is the truncation error of the numerical curve derivation formula of temperature coupling state variables. The smaller the value of λ_i, the smaller the truncation error. The truncation error of the current time point can be reduced by adding interpolation points in the sequential time points. However, the essence of this method is to reduce the iterative time step and increase the number of iterations, which has no substantial effect on improving the iterative efficiency.

The truncation error tolerance range of (2) is denoted as ξ_σ, then following inequality can be obtained from (5):

$$\frac{\lambda_{i+1}\left(\lambda_{i+1}+\lambda_i\right)}{6}\emptyset^{(3)}\left(\xi\right)\leq\xi_\sigma. \tag{6}$$

If $\lambda_{i+1} = a\lambda_i$, then

$$\lambda_i\leq\frac{6\xi_\sigma}{a(1+a)\emptyset^{(3)}\left(\xi\right)}. \tag{7}$$

If $\lambda_{i+1} = \lambda_i$, then

$$\lambda_i\leq\frac{3\xi_\sigma}{\emptyset^{(3)}\left(\xi\right)}. \tag{8}$$

If $\lambda_{i+1} = b\lambda_i$, then

$$\lambda_i\leq\frac{6\xi_\sigma}{b(1+b)\emptyset^{(3)}\left(\xi\right)}. \tag{9}$$

The minimum of the (7)–(9) is taken as the upper limit of CTSP, denoted as $\lambda_{\max}$. If λ_i is excessively small, the state variables of the adjacent steps will cause significant rounding errors due to their similar values. In actual solutions, the rounding error should be lower than the truncation error to avoid the expansion of the error, and λ_i satisfying this criterion defines the lower limit of the time steps, as denoted as $\lambda_{\min}$. $\lambda_{\min}$ can be determined by the physical field analysis tool during the solution. After CTSP is adjusted adaptively, the range of λ_{i+1} needs to be verified before the next simulation cycle. If $\lambda_{i+1} > \lambda_{\max}$, then $\lambda_{i+1} = \lambda_{\max}$. Similarly, if $\lambda_{i+1} < \lambda_{\min}$, then $\lambda_{i+1} = \lambda_{\min}$.

IV. Experiment Validation on Interface-Based Cosimulation

For easier use, an interface software has been developed based on the user interface development tool App Designer, as demonstrated in Fig. 14. The abovementioned software interface development method and coupling strategies are integrated into the software. When performing cosimulation, users do not need to do complex programming work, and only need to make corresponding settings according to the type of study to achieve cosimulation. In the process of cosimulation, the maximum temperature on the device at the end of each iteration is collected by the temperature probe function in MATLAB. After the cosimulation is completed, MATLAB will automatically draw the temperature and power loss distribution profiles according to the results of cosimulation, as illustrated in Fig. 15. Furthermore, the junction temperature fluctuation curve on the chip after the steady state can also be obtained. More detailed postprocessing and analysis, e.g., temperature and mechanical stress, can be performed using the derived thermal or circuit model with the corresponding filename. The stress distribution obtained from the post-processing of the COMSOL model is shown in Fig. 16.

Field-circuit coupling simulations based on the developed interface software and corresponding experimental verification are presented to demonstrate the simulation accuracy and speed of the developed field-circuit coupling interface software.

A. Experimental Setup

To verify the accuracy of the proposed co-simulation method, a customized multichip SiC power module is designed and fabricated, as depicted in Fig. 17. In this phase-leg power module,

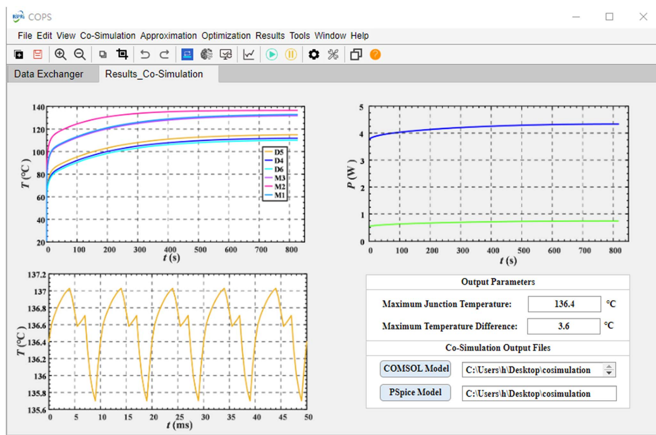

Fig. 15. Software interface of cosimulation results.

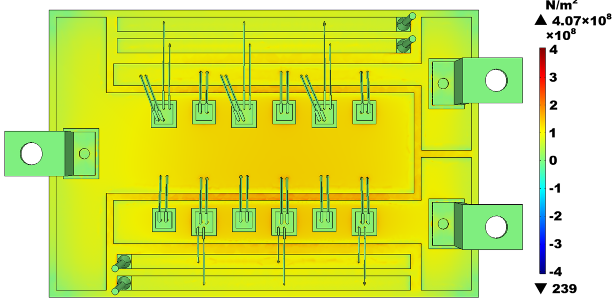

Fig. 16. SiC Power module von Mises stress distribution.

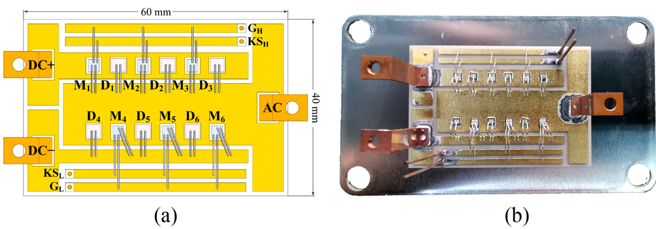

Fig. 17. Designed and fabricated SiC MOSFET power semiconductor module. (a) Chip and terminal location. (b) Manufactured power module.

TABLE I
PACKAGING MATERIALS AND DIMENSIONS

Component	Material	Description
Switch	SiC MOSFET Bare die CPM312000075A	2.5 mm × 2.8 mm Thickness: 0.177 mm
Diode	SiC bare die CPW41200S020B	3.08 mm × 3.08 mm Thickness: 0.377 mm
Substrate	AlN DBC	Area: 60 mm × 40 mm AlN thickness:0.63 mm Cu thickness:0.3 mm
Bonding wire	Al	Diameter:0.254 mm
Die-attach	Sn5-Pb95	Thickness: 0.2 mm
Baseplate	Cu	Area: 104 mm × 59mm Thickness:3.0 mm

Fig. 18. Experimental test rig for evaluating the accuracy of the proposed cosimulation method.

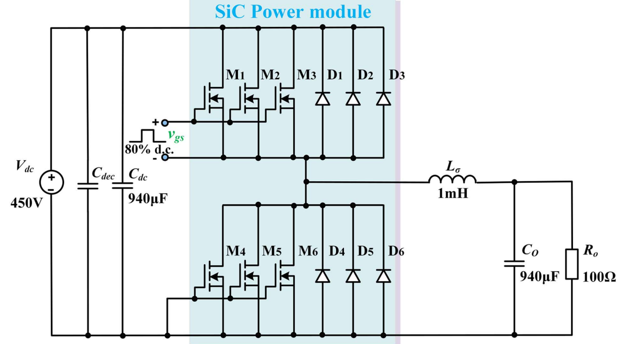

Fig. 19. Schematic of the experimental circuit.

each switch position consists of three parallel connected SiC MOSFET bare dies (CPM312000075A) and three SiC Schottky barrier diodes (CPW41200S020B) from CREE. To conveniently and accurately measure the chip junction temperature, the designed power module is not filled with an encapsulant (silicon gel, epoxy resin) and no case is added. A thin layer of black dielectric coating is sprayed onto the module to increase and unify the surface emissivity. More detailed information about the SiC power module is provided in Table I.

Based on the SiC power module, an experimental test rig for buck circuit in continuous operation is setup, as shown in Fig. 18. The schematic of the experimental circuit is depicted in Fig. 19. M_1, M_2, and M_3 act as active switches, while M_4, M_5, and M_6 are always at OFF state. D_4, D_5, and D_6 act as free-wheeling diodes. M_1–M_3 are driven by a 15 Ω resistor to deliberately increase power losses. The buck converter operates with a 450-V or 400-V dc input voltage, 50-kHz or 100-kHz

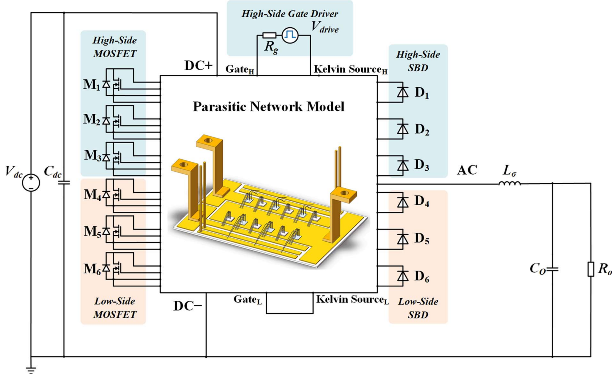

Fig. 20. Circuit simulation diagram with parasitic parameter network.

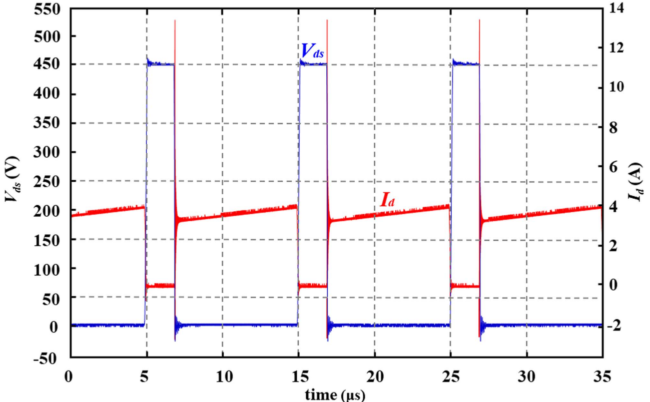

Fig. 21. Experimental switch waveform diagram of SiC MOSFET.

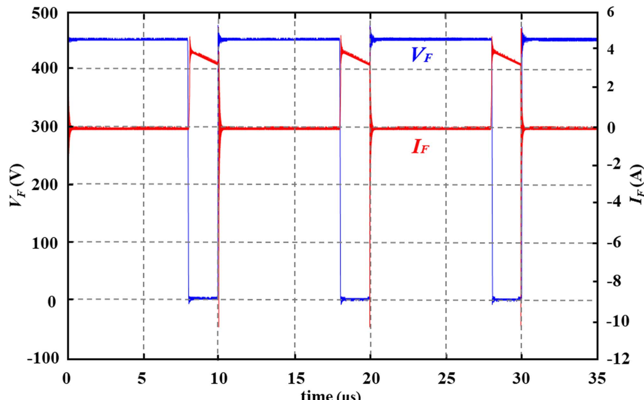

Fig. 22. Experimental switch waveform diagram of diode.

switching frequency, and 0.5 or 0.8 duty cycle. The cooling condition of the converter is natural convection cooling with heatsink, without fan, or liquid coolant. The cosimulation and experimental verification under different cases are performed to fully verify the accuracy of the proposed cosimulation method.

B. Simulation Platform Setup

The field-circuit coupling simulation model consists of two main parts: the circuit simulation model (including the device spice model) and the thermal-mechanical coupling simulation model. These models need to be provided by users and then click the model selection button in the interface software for cosimulation.

In terms of circuit model, the parasitic parameters, including resistance, inductance, capacitance, and conductance (RLCG), can have a great impact on the dynamic and static characteristics of power devices [23], [24]. The parasitic parameters at the device package level can be extracted by performing the quasi-static electromagnetic field simulation leveraging ANSYS Q3D Extractor. The equivalent parasitic network model generated by Q3D is further employed to build a reduced-order lumped circuit model for electromagnetic coupling analysis, as shown in Fig. 20. The initial temperature of the heat source (MOSFET, diode, parasitic resistance) in the circuit is set to 21 °C, which corresponds to the ambient temperature during the experiment. Moreover, the maximum PITS for transient circuit simulation is set to 1-ns to ensure sufficient simulation accuracy. To avoid the heavy computational burden caused by small PITS in the simulation of long time events, the PTSC in each iteration can be greatly shortened to replace the actual one due to the shorter time needed to reach the steady state for circuit simulation. The average power loss calculated from the actual PTSC is consistent with that calculated from the short PTSC.

Regarding the transient thermal-mechanical simulation model, to improve the simulation efficiency and avoid unnecessary calculations, the iterative simulation (except the first iteration) can only give the correct solution at the end of the simulation cycle, and solutions at the intermediate process can be ignored. To ensure that the transient solver performs the calculation and solution strictly at the end of each iteration, the time steps used by the transient solver need to be set to "exact".

C. Accuracy Verification of Field-Circuit Coupling Simulation

The accuracy of the circuit model and the thermal-mechanical model is closely related to the accuracy of the field-circuit coupling simulation. The thermal-mechanical simulation model can achieve relatively high simulation accuracy by modifying material properties and boundary conditions in COMSOL. The accuracy of boundary condition correction, such as the heat dissipation rate of the heatsink, can be verified by comparing the simulation and experimental results in various cases. If the simulation and experimental results under different cases are in good agreement, it can be considered that the boundary condition is set correctly. The accuracy of the switching circuit simulation model heavily relies on how precise the device model is.

Following the same condition shown in Fig. 19 (Case 1), the simulation and experimental results of the buck circuit are shown in Figs. 21, 22, and 23. It is worth noting that the current is the total current flowing through the parallel chips due to the difficulty of measuring the current flowing through a single chip. The comparison results show that differences exist between the simulated switching waveform and the experimental waveform due to the limited accuracy of the spice device model provided by the manufacturer. These differences will lead to some mismatches in power loss between the simulation and experiment.

The average power loss results obtained by the circuit simulation and the experiment are compared in Table II. Due to the

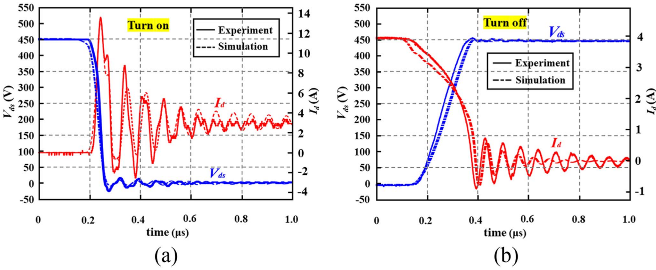

Fig. 23. Simulation and experimental results comparison of switching transition. (a) Turn-ON transition. (b) Turn-OFF transition.

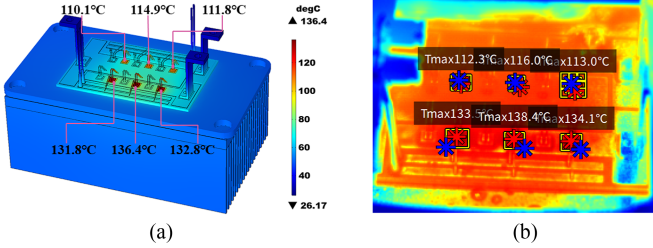

Fig. 24. Steady-state temperature distribution of the power module. (a) Cosimulation result. (b) Experiment result.

TABLE II
COMPARISON OF POWER LOSS RESULTS

Component	Simulation (W)	Experiment (W)
M_1	4.28	4.72
M_2	4.31	4.72
M_3	4.30	4.72
D_4	0.71	0.79
D_5	0.73	0.79
D_6	0.72	0.79

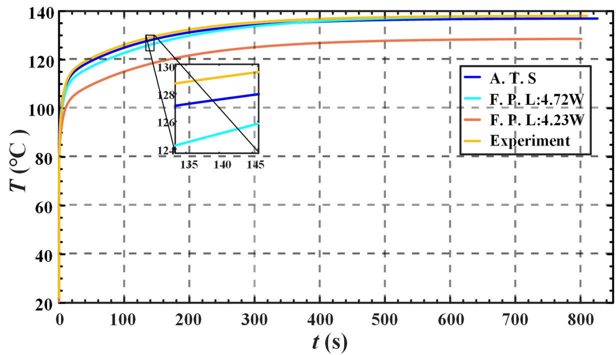

Fig. 25. Transient junction temperature change curve of the chip M_2 in simulation and experiment.

difficulty in current measurement as described previously, it is assumed that the current flowing through each chip is the same, so the power loss of each parallel chip is equal. It can be seen that there is around a 10% mismatch between the experimental and simulated power losses. Simulations and experiments for several other cases also demonstrate that the losses obtained from circuit simulations and experiments are always in error by about 10%. To compensate for the limited accuracy of device models provided by device manufacturers and to avoid complex device modeling efforts, which is beyond the scope of this article, the power loss obtained from the circuit simulation is multiplied by the power loss compensation coefficient τ ($\tau = 1.1$) to make the power loss of the circuit simulation as close as possible to the real one.

On the basis of an accurate circuit model and the thermal-mechanical model, cosimulations under natural cooling conditions are performed to verify the accuracy of the proposed cosimulation method. Taking one of the adaptive time step cases (Case 1) as an example, the corresponding settings are shown in Fig. 19.

The chip temperature distribution obtained by the adaptive CTSP cosimulation method in Case 1 is shown in Fig. 24(a). The steady-state maximum temperature of chips measured by the thermal camera under the same condition is shown in Fig. 24(b). The mismatch between cosimulation and experimental temperature results at steady state is below 2 °C, which is less than 3%.

The transient junction temperature change curve of the chip M_2 (the chip with the highest temperature) obtained from simulation and experimental measurement in Case 1 and that obtained from separate thermal simulation is shown in Fig. 25. It can be seen from the figure that the adaptive time step cosimulation method (A.T.S) proposed in this article agrees well with the experiment in the whole process of simulation (transient change process and final steady state). In the single thermal simulation with fixed power loss input, only when the input power loss data is the power loss data measured at the steady state in the experiment (F.P.L: 4.72 W), the temperature simulation results at the steady state are consistent with those at the steady state in the experiment. There is still a certain error between the simulation results at the transient change process and the experimental results. When the input power loss is not accurate, for example, the input power loss is the power loss calculated by the circuit simulation at room temperature (F.P.L: 4.23 W), the temperature simulation results of the whole process have large errors compared with the experimental results. In summary, compared to the simulation method with fixed loss, the proposed cosimulation method ensures the accuracy of the input power loss at different moments by updating the power loss data in real time. During the cosimulation iteration, the input power loss will dynamically change with the temperature, as shown in Fig. 26. The characteristic that power loss follows the dynamic change of temperature determines that the proposed method has high simulation accuracy in the whole process of simulation.

The transient junction temperature change curve of the chip M_2 in the other three cases measured by the thermal camera PS610 is shown in Fig. 27. The maximum mismatch between the transient cosimulation and experimental results is still within 5%, which verifies the high accuracy of the proposed cosimulation method.

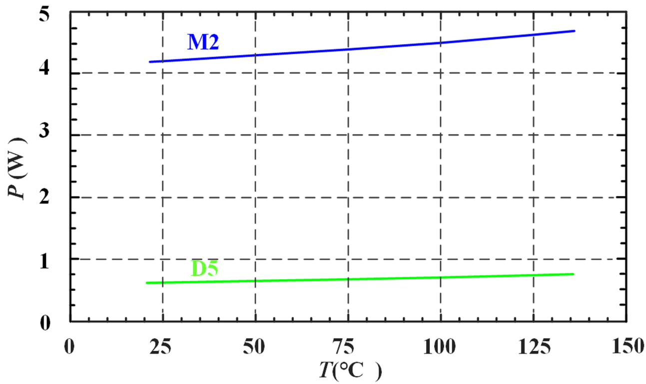

Fig. 26. Graph of input power loss dynamics with temperature.

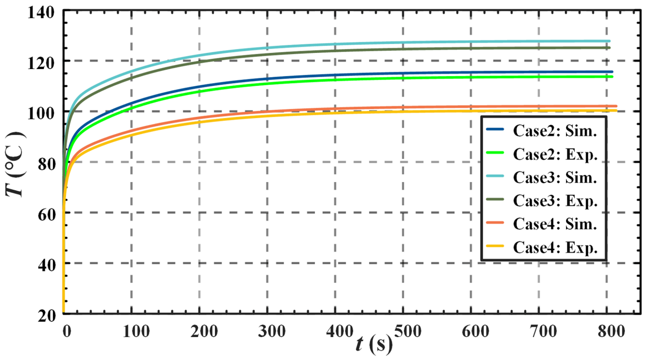

Fig. 27. Variation curve of chip M_2 junction temperature with time obtained by infrared thermal camera and adaptive CTSP cosimulation in other cases. (Case2: 400-V dc input voltage, 100-kHz switching frequency, 0.5 duty cycle; Case3: 400-V dc input voltage, 100-kHz switching frequency, 0.8 duty cycle; Case4: 450-V dc input voltage, 50-kHz switching frequency, 0.8 duty cycle. Sim. stands for simulation while Exp. represents experiment.).

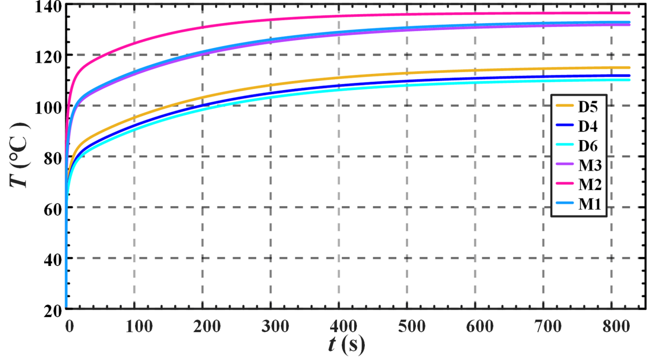

Fig. 28. Variation curve of chip junction temperature with time obtained by cosimulation with the adaptive CTSP.

D. Speed Verification of Field-Circuit Coupling Simulation

The temperature curve of chips obtained by the adaptive CTSP cosimulation following the setup of Fig. 14 in Case 1 is shown in Fig. 28. It can be seen that the absolute slope in the early stage of the temperature curve is relatively large. After two iterative analysis, the derivative $|L_n^{'}(t_i)|$ (MOSFET M_2) stays outside the upper limit of CTSP judgment threshold range. According to the adaptive adjustment strategy, CTSP should be shortened. Since the minimum time step is 0.05 s, the system iteration time step

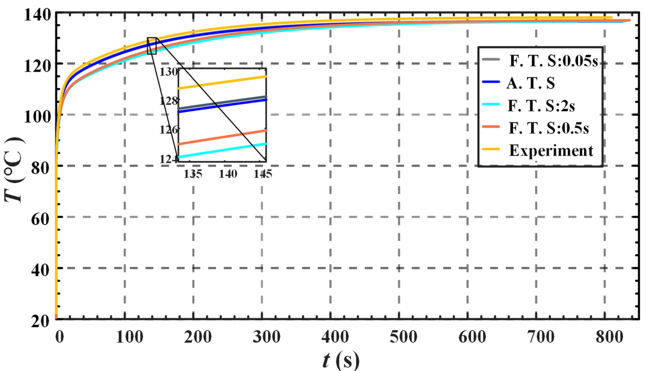

Fig. 29. Variation curve of chip M_2 junction temperature with time obtained by infrared thermal camera and cosimulation in Case 1.

TABLE III
COSIMULATION SOLUTION TIME AND MAXIMUM ERROR

Step size	Simulation time	Maximum error (%)
A. T. S	2h 54min	3.5
F. T. S:0.05	10h 38min	2.7
F. T. S:0.5s	6h 15min	4.1
F. T. S:2s	4h 32min	5.2

is set to the minimum value of 0.05 s. At the end of the 128th simulation iterative cycle, $|L_n^{'}(t_i)|$ falls below the lower limit of CTSP judgment threshold for the first time, causing a growing iteration time step until the maximum CTSP is reached. Then CTSP remains unchanged.

The cosimulation with fixed time step (F.S.) 0.05, 0.5, or 2, respectively, is conducted for comparison purposes. Take the chip M_2 as an example, temperature curves with the adaptive time step (A.S.) sequential coupling method and the fixed time step coupling method are illustrated in Fig. 29. The total cosimulation solution time and maximum mismatch during the transient simulation process are given in Table III. The transient simulations are performed on a computer with 32-GB RAM.

It can be seen from Fig. 29 and Table III that both the adaptive step sequential coupling method and the sequential coupling method with a fixed and small CTSP can effectively solve transient problems. However, the adaptive method dynamically adjusts CTSP and enables a significant improvement in computing efficiency (3–5 times higher). When a fixed and large CTSP is used, despite less time, the accuracy of the transient simulation process is unsatisfactory. The adaptive cosimulation method proposed in this article can achieve a good balance between simulation accuracy and speed.

V. CONCLUSION

In this article, an automated field-circuit coupling simulation software platform is proposed for multichip SiC power module design. It is worth noting that the software platform is also applicable to other power system designs. This software platform provides a software interface that can realize the automatic cosimulation of multisoftware. It helps overcomes the incapability of single simulation software. The developed software interface

adopts an indirect and bidirectional coupling strategy to realize real-time, multirate field-circuit coupling simulation. Moreover, this adaptive time step adjustment strategy can dynamically adjust the CTSP and achieve high simulation accuracy and efficiency simultaneously. Simulation and experiments on a buck converter are conducted to verify the accuracy and efficiency of the interface-based cosimulation approach. The mismatch between cosimulation and experimental results is within 5%, and the simulation efficiency can be improved by 3–5 times.

Future work involves the optimization design of SiC power modules and heatsinks using the proposed multiphysics cosimulation method and artificial intelligence optimization algorithms.

References

[1] F. Yang, Z. Liang, Z. Wang, and F. Wang, “Parasitic inductance extraction and verification for 3D planar bond all module,” in *Proc. IEEE Int. Symp. 3D Power Electron. Integration Manuf.*, 2016, pp. 1–5.

[2] Z. Wang, M. Chinthavali, S. Campbell, T. Wu, and B. Ozpineci, “A 50-kW air-cooled SiC inverter with 3D-Printing enabled power module packaging structure and genetic algorithm optimized heatsinks,” *IEEE Trans. Ind. Appl.*, vol. 55, no. 6, pp. 6256–6265, Nov./Dec. 2019.

[3] Z. Wang, F. Yang, S. L. Campbell, and M. Chinthavali, “Characterization of SiC trench MOSFETs in a low-inductance power module package,” *IEEE Trans. Ind. Appl.*, vol. 55, no. 4, pp. 4157–4166, Jul./Aug. 2019.

[4] B. Du, J. L. Hudgins, E. Santi, A. T. Bryant, P. R. Palmer, and H. A. Mantooth, “Transient electrothermal simulation of power semiconductor devices,” *IEEE Trans. Power Electron.*, vol. 25, no. 1, pp. 237–248, Jan. 2010.

[5] ANSYS Icepak, ANSYS Inc., Canonsburg, PA, USA, 2021. [Online]. Available: https://www.ansys.com/zh-cn/products/electronics/ansys-icepak

[6] Twin Builder Help Document, ANSYS Inc., Canonsburg, PA, USA, 2018. [Online]. Available: https://www.ansys.com/products/digital-twin/ansys-twin-builder

[7] S. Race, A. Philipp, M. Nagel, T. Ziemann, I. Kovacevic-Badstuebner, and U. Grossner, “Circuit-based electrothermal modeling of SiC power modules with nonlinear thermal models,” *IEEE Trans. Power Electron.*, vol. 37, no. 7, pp. 7965–7976, Jul. 2022.

[8] E. Deng, Z. Zhao, Z. Lin, R. Han, and Y. Huang, “Influence of temperature on the pressure distribution within press pack IGBTs,” *IEEE Trans. Power Electron.*, vol. 33, no. 7, pp. 6048–6059, Jul. 2018.

[9] K. B. Pedersen and K. Pedersen, “Dynamic modeling method of electro-thermo-mechanical degradation in IGBT modules,” *IEEE Trans. Power Electron.*, vol. 31, no. 2, pp. 975–986, Feb. 2016.

[10] J. Wang et al., “A transient 3-D thermal modeling method for IGBT modules considering uneven power losses and cooling conditions,” *IEEE J. Emerg. Sel. Topics Power Electron.*, vol. 9, no. 4, pp. 3959–3970, Aug. 2021.

[11] Z. Zeng, X. Zhang, F. Blaabjerg, H. Chen, and T. Sun, “Stepwise design methodology and heterogeneous integration routine of air-cooled SiC inverter for electric vehicle,” *IEEE Trans. Power Electron.*, vol. 35, no. 4, pp. 3973–3988, Apr. 2020.

[12] Isight Help Document, Dassault Systemes Inc., PA, France, 2021. [Online]. Available: https://www.3ds.com/zh/products-services/simulia/products/isight-simulia-execution-engine/

[13] R. Wu et al., “A temperature-dependent thermal model of IGBT modules suitable for circuit-level simulations,” *IEEE Trans. Ind. Electron.*, vol. 52, no. 4, pp. 3306–3314, Jul./Aug. 2016.

[14] R. Wu, F. Iannuzzo, H. Wang, and F. Blaabjerg, “An Icepak-PSpice cosimulation method to study the impact of bond wires fatigue on the current and temperature distribution of IGBT modules under short-circuit,” in *Proc. IEEE Energy Convers. Congr. Expo.*, 2014, pp. 5502–5509.

[15] Y. Jia, F. Xiao, Y. Duan, Y. Luo, B. Liu, and Y. Huang, “PSpice-COMSOL-based 3-D electrothermal–mechanical modeling of IGBT power module,” *IEEE J. Emerg. Sel. Topics Power Electron.*, vol. 8, no. 4, pp. 4173–4185, Dec. 2020.

[16] W. Wang, H. R. Wickramasinghe, K. Ma, and G. Konstantinou, “Real-time co-simulation for electrical and thermal analysis of power electronics,” in *Proc. IEEE 9th Int. Conf. Power Energy Syst.*, 2019, pp. 1–5.

[17] B. Gao et al., “A temperature gradient-based potential defects identification method for IGBT module,” *IEEE Trans. Power Electron.*, vol. 32, no. 3, pp. 2227–2242, Mar. 2017.

[18] T. Funaki, “Modeling and model parameter extraction of wide bandgap power semiconductor device, package, and circuit for simulating fast switching behavior,” in *Proc. IEEE Energy Convers. Congr. Expo.*, 2019, pp. 2181–2185.

[19] Y. Chen, W. Li, F. Iannuzzo, H. Luo, X. He, and F. Blaabjerg, “Investigation and classification of short-circuit failure modes based on three-dimensional safe operating area for high-power IGBT modules,” *IEEE Trans. Power Electron.*, vol. 33, no. 2, pp. 1075–1085, Feb. 2018.

[20] Z. Wang, “Study on the method of modelling and simulating of complex electro-mechanical system,” *Mater. Sci. Forum.*, vol. 963, pp. 1–5, Nov. 2003.

[21] M. Bayer, S. Hartmann, M. Berg, R. Moody, and G. Paques, “Interpretation of power cycling data derived from transient cooling curves,” in *Proc. IEEE 10th Int. Conf. Integration Power Electron. Syst.*, 2018, pp. 1–6.

[22] G. Xin, J. Peng, and Z. Jun, “Research on DYC of EV based on virtual prototype and collaborative simulation platform,” *J. Syst. Simul.*, pp. 2338–2344, 2008.

[23] F. Yang, Z. Wang, Z. Zhang, S. L. Campbell, and F. Wang, “Analysis and experimental evaluation of middle point inductance’s effect on switching transients for multiple-chip power module package,” *IEEE Trans. Power Electron.*, vol. 34, no. 7, pp. 6613–6627, Jul. 2019.

[24] Z. Wang, F. Yang, S. Campbell, and M. Chinthavali, “Development of a low-inductance SiC trench MOSFET power module for high-frequency application,” in *Proc. IEEE Appl. Power Electron. Conf. Expo.*, 2018, pp. 2834–2841.

Yayong Yang (Student Member, IEEE) was born in Henan, China. He received the B.S. degree in electrical engineering from Hunan University, Changsha, China, in 2020. He is currently working toward the Ph.D. degree in artificial intelligence with the Huazhong University of Science and Technology, Wuhan, China.

His current research interests include packaging and integration of SiC power modules, and application of artificial intelligence in power electronics.

Zhiqiang (Jack) Wang (Senior Member, IEEE) received the B.S. degree from Hunan University, Changsha, China, in 2007, and the M.S. degree from Zhejiang University, Hangzhou, China, in 2010, both in electrical engineering, and the Ph.D. degree in electrical engineering from the University of Tennessee, Knoxville, TN, USA, in 2015.

He is currently a Full Professor with the Huazhong University of Science and Technology (HUST), Wuhan, China. Prior to joining HUST, he was with the Power Electronics and Electric Machinery Research Center, Oak Ridge National Laboratory (ORNL), Oak Ridge, TN, USA, as a Postmaster Research Associate, from 2014 to 2015, a full-time R&D Associate Staff Member, from 2015 to 2018, and an R&D Staff Member in 2019. He has also been an Adjunct Professor with the University of Tennessee since 2018. He has authored and coauthored more than 80 publications in international conferences and journals. His research interests include packaging and integration of wide bandgap power semiconductor devices, and its applications to high temperature, high frequency, and high-density power electronics systems.

Dr. Wang was the recipient of more than 10 awards from ORNL and IEEE. He was the Technical Program Chair for WiPDA-Asia 2021 conference and is currently the Transaction Paper Review Chair for the IEEE IAS Power Electronics Devices and Components Committee.

Yuxin Ge (Student Member, IEEE) was born in Anhui, China. She received the B.S. degree from Chongqing University, Chongqing, China, in 2020, and the M.S. degree from Huazhong University of Science and Technology, Wuhan, China, in 2023, both in electrical engineering.

Her research interests include packaging and integration of SiC power semiconductor modules, and parallel operation of SiC MOSFETS.

Guoqing Xin (Member, IEEE) received the B.S. degree in chemistry from Shandong University, Jinan, China, in 2009, the M.S. degree in chemical engineering from Sungkyunkwan University, Suwon, South Korea, in 2011, and the Ph.D. degree in mechanical engineering from Rensselaer Polytechnic Institute, Troy, NY, USA, in 2016.

He is currently a Full Professor with the Huazhong University of Science and Technology (HUST), Wuhan, China. Prior to joining HUST, he was with Global Foundries, as a Senior Process Engineer, from 2017 to 2019. He was a Postdoctoral Researcher with Rensselaer Polytechnic Institute, Troy, NY, USA, from 2016 to 2017. He has authored and coauthored more than 40 technical papers in journals and conference proceedings. His research interests include wide bandgap semiconductor devices fabrication, thermal management of power electronics, and high temperature modules for power electronic applications.

Xiaojie Shi (Senior Member, IEEE) received the M.S. degree from Zhejiang University, Hangzhou, China, in 2011, and the Ph.D. degree from the University of Tennessee, Knoxville, TN, USA, in 2015, both in electrical engineering.

She is currently a Full Professor with the Huazhong University of Science and Technology (HUST), Wuhan, China. Prior to joining HUST, she was with the Center for Ultra-Wide-Area Resilient Electric Energy Transmission Networks, University of Tennessee, Knoxville, TN, USA, as a Research Assistant Professor in 2016, and with the Electric Power Research Institute, Knoxville, TN, USA, as an Engineer/Scientist II, from 2017 to 2019, and Engineer/Scientist III from 2020 to 2021. Since 2019, she has also been an Adjunct Professor with the University of Tennessee, Knoxville, TN, USA. She has authored/coauthored more than 60 publications in international conferences and journals. Her research interests include driving and protection of power semiconductor devices, modeling, and control of grid-connected power converters, microgrid design, and operation.